

Modal identification of damaged frames

Mariella Diaferio^{1,*},† and Vincenzo Sepe²

¹*Department of Sciences in Civil Engineering and Architecture, Technical University of Bari, Via Re David 100, I-70125 Bari, Italy*

²*Department of Engineering and Geology, University "G. D'Annunzio" of Chieti-Pescara, Viale Pindaro 42, I-65127 Pescara, Italy*

SUMMARY

The paper investigates the possibility of identifying localised damages for multi-span and multi-floor linear elastic frames using only natural frequencies measured in the undamaged and damaged configurations. Namely, frames of increasing complexity are studied by exploring one by one their significant substructures (i.e. multi-span beams, floor by floor); the error function is defined and minimised on a database of finite element damaged models that only includes the natural frequencies of the local modes of the substructure, that is, the only modes significantly affected by the localised damage considered here. The performances and limits of the procedure are here discussed by means of numerical simulations on steel frames of increasing complexity; a particular attention is also devoted to the role of noise on the identification procedure. Copyright © 2015 John Wiley & Sons, Ltd.

Received 4 March 2014; Revised 13 March 2015; Accepted 5 May 2015

KEY WORDS: damage identification; multi-span and multi-floor linear elastic frames; natural frequencies; global and local modes; substructures

1. INTRODUCTION

As it is well known, the dynamic parameters of a structure are strictly dependent on its mechanical and geometrical characteristics; many studies have therefore been devoted to the inverse dynamical problem, that is, the evaluation of the dynamical parameters – as modal parameters in the case of linear behaviour – and then of the structural characteristics on the base of the recorded vibrations of the structure. Indeed, the main advantage of this procedure is that low intensity – and therefore not destructive – dynamical tests can give satisfactory results, and in the case of dynamical identification procedure with unknown input, they can be performed also during ordinary service conditions [1–18].

Another advantage of the dynamical identification is the possibility to obtain a reliable finite element (FE) model by updating a less refined one, until a satisfactory matching is obtained between its numerical results with the real experimental response [19–24]. In the field of dynamical identification procedures, many studies deal with the problems connected to damage detection [25–44]. The proposed techniques are based on the obvious observation that the damage is responsible of a stiffness reduction of the structure (in some cases also variations of the masses and damping are expected); as a consequence, the damage, even if localised in one or few sections, may produce variations of structural dynamical parameters (modal shapes, frequency values, etc.) that, in turn, can allow to identify damage position and severity, as it is shown in the aforementioned studies. Nevertheless, the research is still in progress to define identification techniques that, depending on the kind of considered structure and damage, guarantee a good accuracy with a reasonable experimental effort, and also recently, many new methods have been proposed which use different approaches.

*Correspondence to: Mariella Diaferio, Department of Sciences in Civil Engineering and Architecture, Technical University of Bari, Via Re David 100, I-70125 Bari, Italy.

†E-mail: mariella.diaferio@poliba.it

One of the most recent approaches makes use of the wavelet analysis [25–28] for the identification of structural damage. Namely, in [25], Basu demonstrates that, in case of stiffness degradation of a mass–spring system, the wavelet coefficients allow to infer if the system is damaged or not, even in the absence of any information about the undamaged structure.

In [28], the reliability of a real-time identification technique based on the wavelet analysis for the identification of stiffness variations is discussed. The use of the wavelet technique to identify structural damage is further investigated in [27], where the availability of output-only records is explored by means of numerical simulations and experimental tests on a three-storey structure; it is shown that the wavelet technique allows a very effective detection of frequency changes because of damage, so allowing to infer the damage occurrence even without any information on the external excitation.

Some Authors have also focused their attention on the experimental validation of the use of wavelet analysis for the damage detection. In [26], in the case of shaking table tests simulating earthquakes loads on concentrically-braced steel frames, it was shown that a wavelet analysis allows to detect the yielding (for tensile stresses) and the buckling (for compressive stresses) of brace members, once few records of the acceleration time histories (input and output) are available.

Other approaches are based on the definition of a damaged finite element model, obtained by modifying the undamaged one (model updating) in order to match the experimental response of the damaged structure. In this field, some Authors have performed wide experimental campaigns for the validation of such damage detection techniques, as in [29], where a full-scale seven-storey reinforced concrete shear wall building has been subjected to shaking table tests.

This approach has been also adopted for detecting damage in structures in which the locations of plastic phenomena can be predicted (a high-ductile steel–concrete composite frame in [30] and a steel–concrete moment-resisting frame in [31]). However, the required experimental setup is burdensome as the sensors have to be installed in order not only to measure the global response of the structure but also the local response of the possible portions in which the damage is expected.

Other numerous methods have also been proposed and experimentally validated as the damage index method and the damage location vectors method [32], or the method that analyses the changes of the stiffness and damping matrices [33] for multi-floor frames, or the modal curvature in case of a masonry arch [34]; however, all such procedures require the evaluation of modal shapes, which implies a high experimental effort.

To reduce such an effort, several Authors (e.g. [35]) have investigated the possibility of identifying the damage taking into account incomplete measured mode shapes and frequencies or have proposed the use of experimentally measured frequency response functions as in [36].

Indeed, for practical application of the numerous and different approaches available, a crucial role is played by the experimental setup, which should be as simple and reliable as possible.

In order to simplify the experimental setup, a possible solution is given by procedures for structural damage identification that requires only the knowledge of the natural frequencies that can be cheaply and accurately estimated; a review of such frequency-based methods is presented in [37].

In [38], the effectiveness of two damage detection methods (one based on the flexibility variations and the other one on the natural frequencies variations), analysing two complex steel frames subjected to shaking table tests, is investigated. The authors demonstrate that the use of natural frequencies shifts can allow to detect the damage only if multiple modes are taken into account.

More recently, in [39,40], the position and severity of a localised damage is identified by using a data base of FE models simulating any possible position and level of damage in a given range for a one-span-one-floor frame or an arch.

In [41,42], the writers have shown the effectiveness of the previous method for analysing the damage in a two-span beam by means of experimental tests (details in [42]).

However, as the complexity of the structure increases, the difficulties in the damage identification correspondingly increase, and the definition of an effective method is still on debate. In fact, the local variation of stiffness, as for damage examined in this paper, does not produce significant variations of the natural frequencies related to global modes in large-scale structures, and consequently, these methods cannot guarantee correct damage detection.

The present paper deals with these problems and investigates the possibility of identifying localised damages for multi-span and multi-floor linear elastic frames using only natural frequencies measured in

the undamaged and damaged configurations. Indeed, in case of low excitations, as those considered here, the procedure takes into account the ‘local’ modes that are more sensitive to localised damage.

The identification can in fact be effective only if the recorded data allow to extract dynamical parameters significantly affected by damage, and in the case of very simple structures (e.g. a one-span-one-floor frame or an arch), the identification of the first natural modes (or even of the modal frequencies only, as shown in [39,40]) can be appropriate for damage identification.

On the other hand, in complex structures (e.g. multi-span and multi-floor frames), damage generally affects significantly only higher modes; in these cases, the ambient actions that excite first modes only are not adequate as forcing loads [41–43], and the dynamical tests have to be performed by applying external forces, that is, impulsive forces at the same floor of the damaged beam.

The higher modes taken into account in the method discussed here are selected by applying a substructure approach that explores one by one significant substructures [41,42], namely multi-span beams of a given frame, floor by floor. In this way, the error function is defined and minimised on a database of damaged FE models that includes only the natural frequencies of ‘local modes’, that is, modes that mainly imply deformations of a given substructure, which are the only modes significantly affected by the localised damage considered here.

The basic aspect of the procedure is described in Section 2. Section 3 describes the numerical investigations on a 2×2 steel frame (two floors and two spans, Section 3.2) and on a 3×3 steel frame (three floors and three spans, Section 3.3), including two alternative ways of dealing with the random noise, showing the practical applicability of the proposed procedure.

As the complexity of the structure increases, the selection of the modes that have to be taken into account may request a more systematic approach as, for example, the evaluation of a sensitivity matrix as proposed in [44].

2. DAMAGE DETECTION

2.1. Minimisation procedure for the damage detection in complex structures

According to [27], damage identification can be performed at different levels: level 1 techniques only allow to detect the occurrence of a damage, while level 2 and level 3 techniques also allow to identify the position of the damage and the time instant of its occurrence, respectively. The present paper deals with a level 2 technique, that is, the estimation of the position and level of damage in the case of a structure with a notch localised in a single section. In this case, differently from the ‘breathing crack’ (opening and closing of a crack in the vibrating process, see for example [45–47]) that implies a discontinuous and therefore nonlinear behaviour, it can be assumed a linear behaviour even for the damaged structure and the classical procedures for frequency identification can be applied.

As aforementioned, it has been chosen to perform the damage detection by using the natural frequencies of the structure that, as well known, have the advantage of being less affected by noise and can be more accurately evaluated also with lower experimental effort. Nevertheless, it can be difficult (or even impossible) to detect localised damage in a complex structure by observing frequency (or shape) modification of global modes, which are often negligible. This motivated the substructure approach discussed here that uses only a selected set of higher modes, as the effects of damage are more relevant on ‘local’ modes of the substructure affected by damage, provided that local excitations on this part of the structure are applied [41,42].

For identifying position and intensity of damage, the procedure needs a reference finite element model (FEM), calibrated through a modal updating by means of undamaged experimental frequencies, and a database of varied FE models, obtained by considering different positions and levels of damage in a significant range.

The damage can be identified by introducing an error function based on the experimentally evaluated variations of an appropriate number of natural frequencies between damaged and undamaged configurations; the experimental variations are compared with the corresponding numerical ones obtained through the aforementioned FE models of the undamaged and damaged states.

A similar error procedure, but implemented considering the ‘classical’ global modes, has been investigated in [41–43] by performing experimental tests on a two-span beam, and in this case, it has

been shown that the damage is detected with good accuracy; nevertheless, the application of this procedure on more complex structures was only tested for a simple frame and a systematic approach to take into account the measurement noise was not investigated. To overcome these limitations, the approach proposed in the succeeding sections, which adopts a modified error function coherent with the use of ‘local’ modes of substructures and a procedure for improving the accuracy in the presence of noise, proves to be effective for frame structures. In detail, the identified solution (position s and depth p of the notch, modelled as a rotational spring, see Section 2.2) corresponds to the minimum of the error function:

$$G(s, p) = \sum_{i=1}^N \left((\omega_i^D - \omega_i^U) - (\omega_{i,e}^D(s, p) - \omega_{i,e}^U) \right)^2 \tag{1}$$

where N is the number of natural modes taken into account, ω_i^U and ω_i^D denote the measured undamaged and damaged i -th natural frequencies, $\omega_{i,e}^U$ is the i -th frequency of the undamaged FE model and $\omega_{i,e}^D(s, p)$ denotes the i -th frequency of the FE model with a damage at position s and level p .

Indeed, the identification of damage on a given substructure (e.g. the multi-span beam of a given floor of a frame) is mainly influenced by higher frequency ‘true local’ modes (i.e. modes that include deformations localised in the investigated substructure) more than by ‘global’ modes of the structure as a whole. For this reason, the use of absolute frequency changes, as here introduced as in Eqn 1, preserves the effective weight of the local modes in the error function, while the normalisation used in

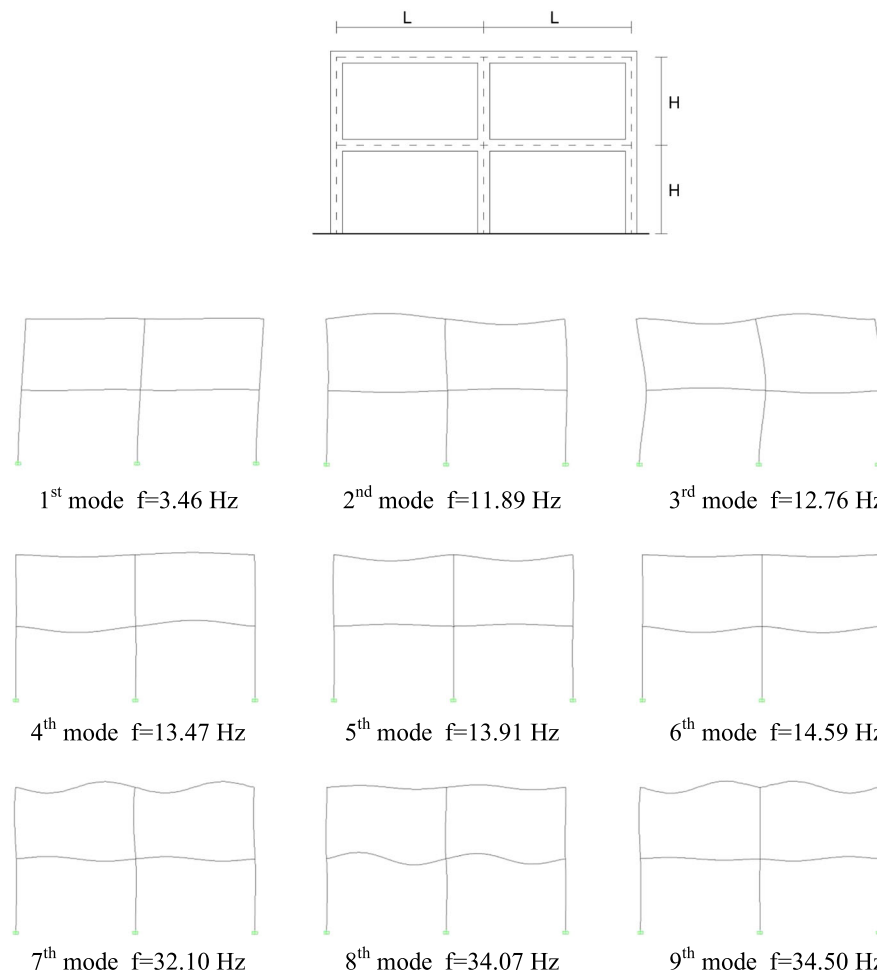


Figure 1. First line: steel frame of Section 3.1: $L=5$ m, $H=3$ m, columns HE 400B and beams IPE 400. Bottom: first nine natural modes of the undamaged frame.

[39,41,42], which divides each term of the error function by the corresponding modal frequency, penalises the contribution of higher frequency modes, namely, the local modes that are more sensitive to a damage in the considered substructure.

This identification technique implies a relatively small computational effort for multi-span beams, but for an increasing structural complexity, the computational burden may be relevant and even prohibitive; to this respect, algorithms to generate automatically the FE database should be implemented, as it will be tried in the future.

The problem of modal density also arises when the structural complexity increases (e.g. passing from single or multi-span beams to multi-floor and multi-span frames); in this case, structural modes with close natural frequencies have to be examined to select the only ones that can be really detected and used for identification purposes, that is, those significantly excited by the local forces applied to a given substructure.

In the numerical examples discussed in the succeeding sections, the selection of the natural modes of the FE 'damaged' models to be included in the database for minimisation procedure has been performed directly by visually exploring the modal shapes; of course, an algorithm to perform the modes selection automatically is mandatory to extend the procedure to more complex (and more significant) structures; for example, systematic approach for the selection of the modes has been proposed in [44], which makes use of the evaluation of a sensitivity matrix.

With reference to the experimental setup, the substructure approach requires a lower experimental effort with respect to the installation of sensors on the whole structure, considered that only the modes excited by local actions on a given substructure have to be identified. In this case, of course, the procedure of local forcing and data recording must be repeated on the other substructures, one by one, even if a detailed location of sensors can be extended to the whole structure (that indeed is unusual for practical or economic reasons). In any case, even if low-cost sensors could be diffusely placed on the whole structure, the proposed approach requires to apply an impulsive load on a selected part of the frame (substructure) and then to repeat the procedure for each significant part of the structure.

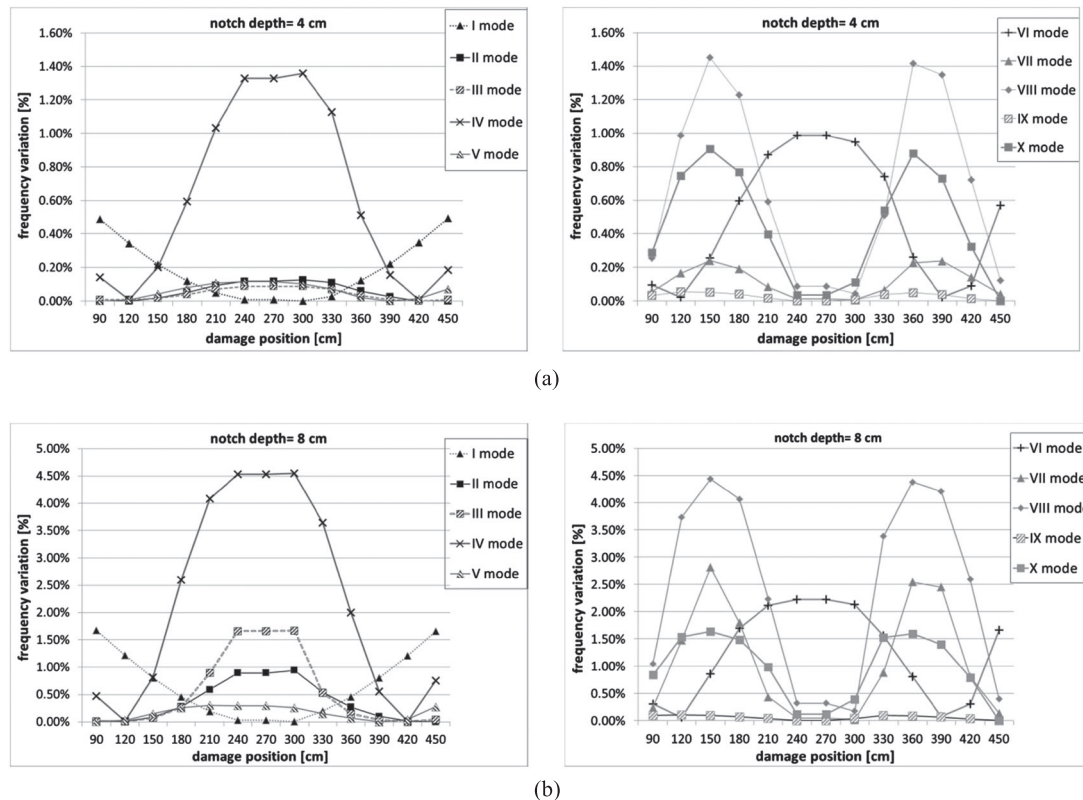


Figure 2. Frequency variation of the first 10 natural modes with respect to the undamaged frame of Figure 1 versus position of damage: (a) notch depth equal to 4 cm and (b) notch depth equal to 8 cm.

2.2. The model of damage

In the present paper, the damage is modelled as a notch localised in a single section of the structure. In accordance with Chondros *et al.* [48] and the papers there quoted, the damage is introduced in the FE model of the structure through a rotational spring connecting the undamaged parts, with a stiffness k defined as follows:

$$k = \frac{EI}{6\pi(1 - \nu^2)h\Phi_1} \tag{2}$$

where E is the elastic modulus, ν is the Poisson coefficient and I and h are the moment of inertia and the height of the beam section, respectively; according to Chondros *et al.* [48], the non-dimensional coefficient Φ_1 depends on the ratio α between the notch depth p and the beam thickness h

$$\Phi_1 = 0.6272\alpha^2 - 1.04533\alpha^3 + 4.5948\alpha^4 - 9.9736\alpha^5 + 20.2948\alpha^6 - 33.0351\alpha^7 + 47.1063\alpha^8 - 40.7556\alpha^9 + 19.6\alpha^{10} \tag{3}$$

This damage model is used in the paper to define a sufficiently wide set of FE models of the structure, varied with respect to the undamaged one by considering different positions and levels of the damage in a given range. The eigenvalue analysis of these models allows to build a database collecting the frequency values of the significant natural modes for each damaged configuration.

It is worth noting that the described procedure can be applied also if a different damage model is available, for example, based on experimental tests for the material and particular characteristics of the examined frame.

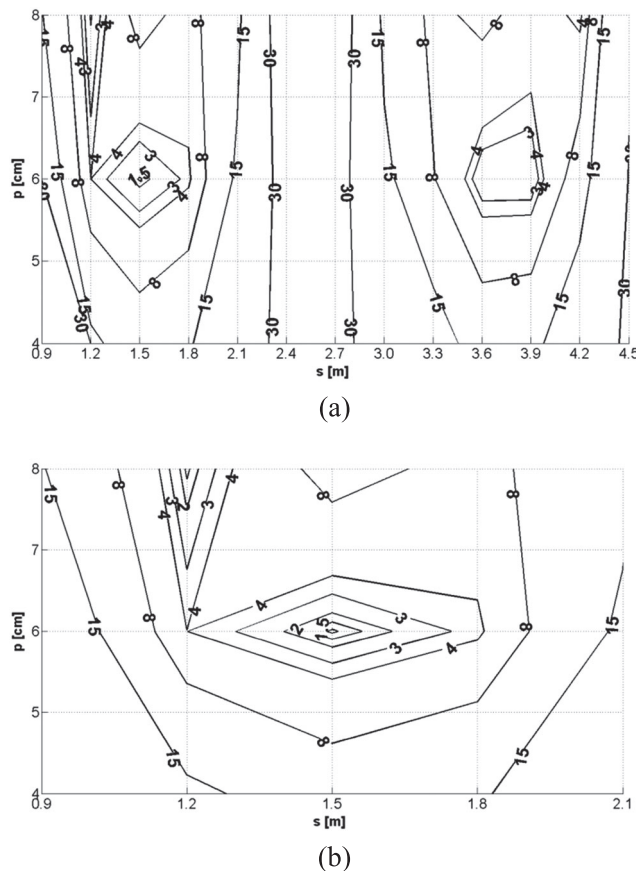


Figure 3. Level curves of the error function G/G_{min} for the frame in Figure 1; pseudo-experimental data generated with damage $s = 1.5$ m and $p = 6$ cm; added ‘noise’ $\pm 30\%$ of the difference between damaged and undamaged frequencies. (a) Plot for all the possible damage position and (b) zoom nearest the minimum point.

3. NUMERICAL INVESTIGATION ON PLANE FRAMES

3.1. Sample case #1: two-span and two-floor steel planar frame

In this section, the analysis of the steel frame in Figure 1 is described. The FE model of the frame has been developed assuming 7850 kg/m^3 for the mass density, 0.3 for the Poisson coefficient and $2 \times 10^5 \text{ MPa}$ for the elastic modulus. A non-structural mass, deriving from distributed loads on the beams, is also added to the mass of the structural elements of the frame. In detail, a load of 28 kN/m has been added to the structure. Moreover, the columns have been assumed fully fixed at the base and the beam–column connections as rigid, while the damping coefficient is equal to 0.5%.

The analysis has been performed assuming that the damage, represented by a notch in a section without significant reduction of the beam mass, is localised in only one transversal section of the beam at the first floor. On the base of this hypothesis, the FE database has been built varying damage position on the beam at the first floor with a step $\Delta s \approx 30 \text{ cm}$ (1/16 span) and ranging the notch depth between 1 and 8 cm (four different levels of damage have been considered), and evaluating the first 10 natural modes. As a consequence, taking into account the symmetry of the frame, the database consists of 680 elements, corresponding to 68 different damaged configurations of the frame.

In Figure 1, the modal shapes and frequencies of the first nine natural modes of the undamaged structure are shown. As it can be easily verified, the first and third modes correspond to the ‘global’ modes, while the others are ‘local’ modes.

In Figure 2, the differences between the frequencies of the first 10 natural modes of the damaged configurations and the undamaged one, normalised with respect to the undamaged frequencies, are plotted as a function of the position of damage (distance from the left end of the beam) and for different notch depth levels. The plots in Figure 2 confirms that, for the case here considered, the natural frequencies of higher modes (i.e. ‘local’ modes) are more sensitive to damage than the ‘global’ modes,

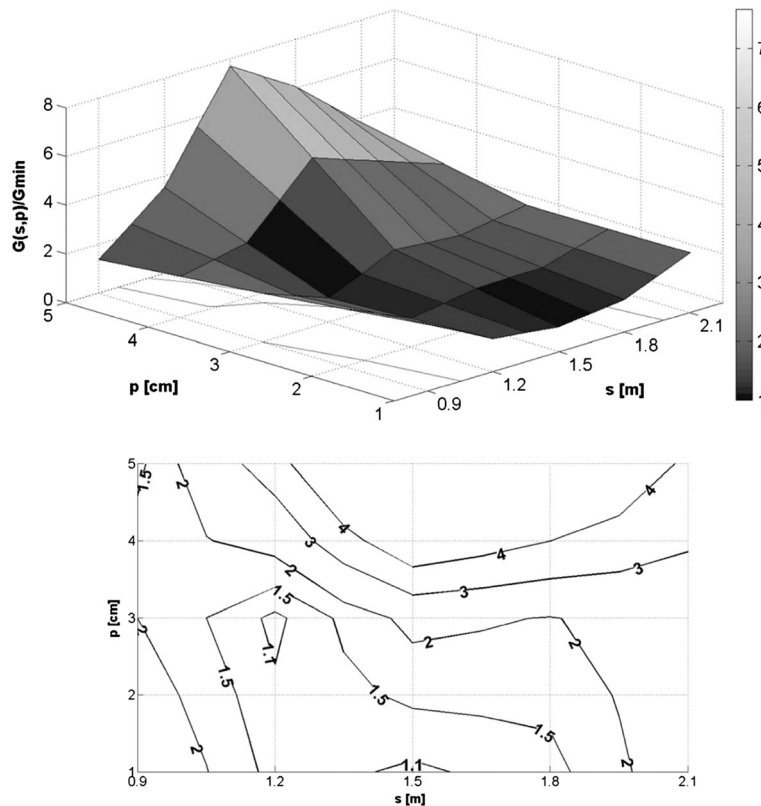


Figure 4. Error function G/G_{min} (top) and level curves (bottom) for the frame in Figure 1, pseudo-experimental data generated with damages $s = 1.5 \text{ m}$ and $p = 3 \text{ cm}$; added ‘noise’ $\pm 30\%$ of the difference between damaged and undamaged frequencies.

and some of them show a frequency variation three to five times larger than the values related to the ‘global’ modes.

Quite obviously, the frequency variations are strongly influenced by damage position; as a consequence, the accuracy of the damage detection procedure depends on the combination of considered modes.

For these reasons, and because of the errors and uncertainties connected to modal analysis, the writers suggest to perform the damage detection considering at least the first five to six identified ‘local’ modes, as it has been performed here.

To evaluate the performance of the method, three damaged configurations have been investigated with pseudo-experimental (i.e. numerically generated) data. In detail, with reference to the frame in Figure 1, three damaged configurations have been considered: (i) a notch with 6-cm depth at 1.5 m from the left end of the first-floor beam; (ii) a notch with 3-cm depth at 1.5 m from the left end of the first-floor beam; and (iii) a notch with 6-cm depth at 2.1 m from the left end of the first-floor beam.

The acceleration time histories have been numerically generated [41,42] by means of a finite elements model of the frame (pseudo-experimental data), under an impulsive load at 2/3 of the left span, with a distance between ‘measurements’ points equal to 1/8 of the span. The simulated data have then been processed to get significant modal frequencies.

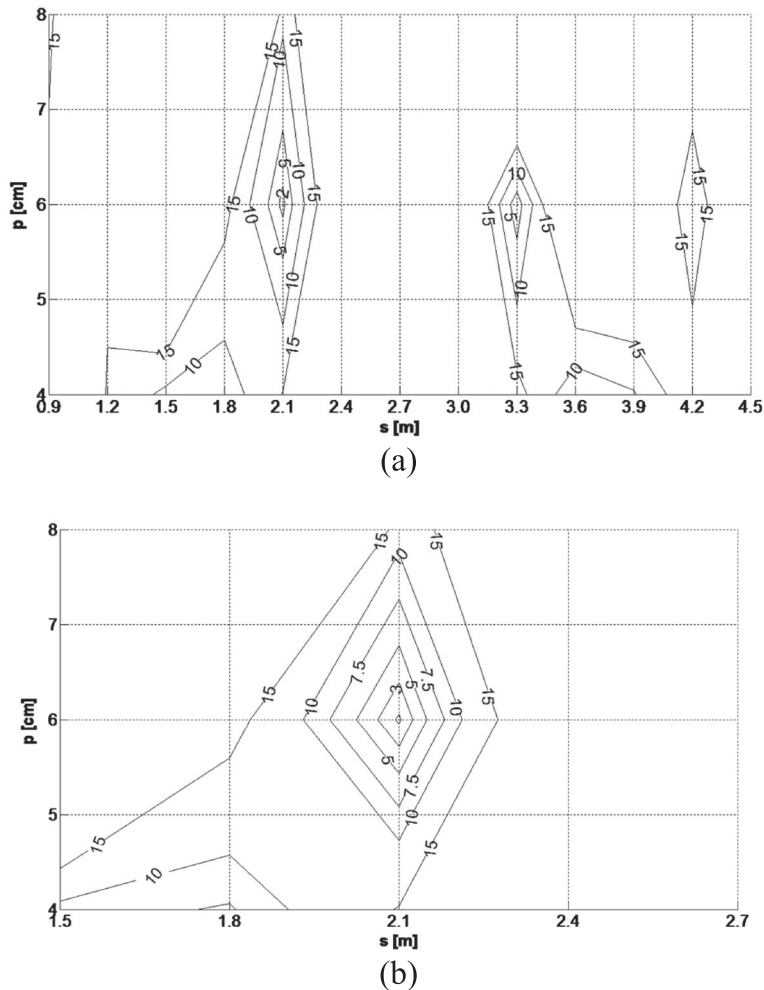


Figure 5. Level curves of the error function G/G_{min} for the frame in Figure 1, pseudo-experimental data generated with damage $s = 2.10$ m and $p = 6$ cm. The analysis has been performed taking into account the 1st, 4th and 8th modes. (a) Plot for all the possible damage position and (b) zoom nearest the minimum point.

As usual, in practical cases the experimental undamaged model has to be obtained by model updating of a tentative FE model, while here the reference numerical model has obviously been considered.

According to the results shown in Figures 3 and 4, the procedure provides a satisfactory identification of damage even for this kind of structures. For the configuration #1 described in Figure 3, it is observed in fact a good accuracy for the location and intensity of damage, even if a ‘noise’ is added to the modal frequencies of the damaged case to roughly simulate experimental data; namely, an error has been added to damaged frequencies, ranging between $\pm 30\%$ of the difference between damaged and undamaged values. Quite obviously, for a decreasing severity of damage, the accuracy of the identification decreases, as shown in Figure 4 (configuration #2, $s = 1.5$ m, $p = 3$ cm), where the position of damage can be only roughly estimated.

In Figures 5 and 6, the results of the damaged configuration #3 are shown. In this case, the analysis has been performed taking into account two different selection of modes: Figure 5 shows the level curves of the error function obtained considering only the first, third and sixth identified modes that correspond to the first, fourth and eighth modes of FE model of the frame, and Figure 6 shows the same level curves evaluated performing the procedure with reference to the first six identified modes that correspond to the first, second, fourth, sixth and eighth modes of the FE model. It can be observed that in this case, the good accuracy of the method is guaranteed also with only three local modes, although no general conclusion can be derived from this sample case.

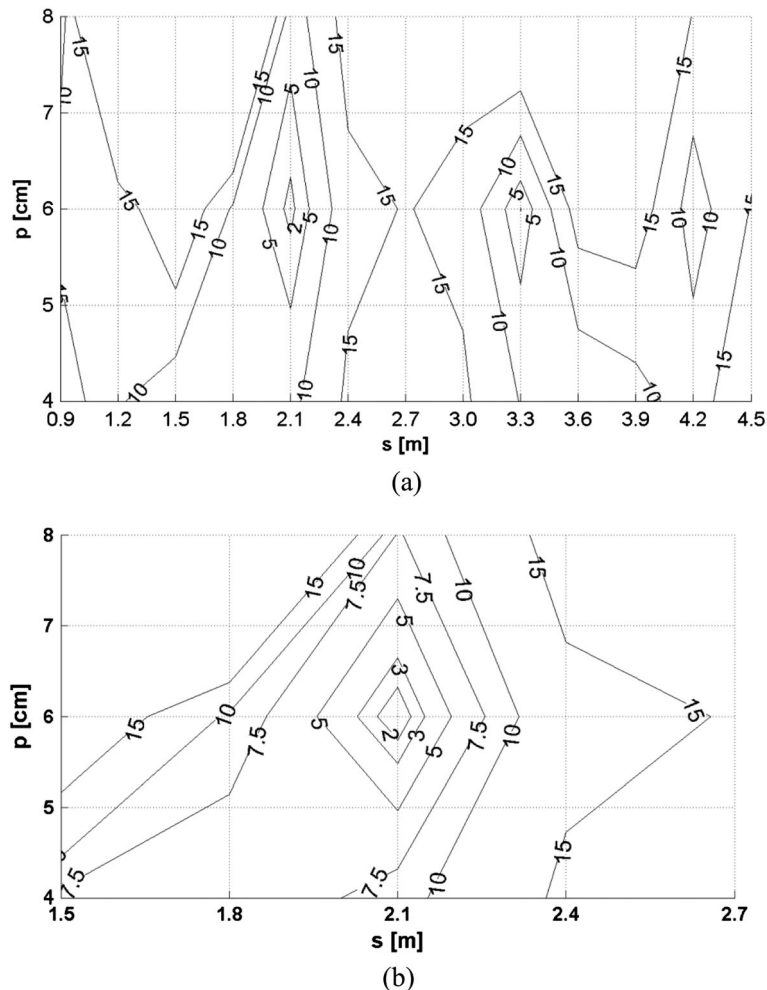


Figure 6. Level curves of the error function G/G_{min} for the frame in Figure 1, pseudo-experimental data generated with damage $s = 2.10$ m and $p = 6$ cm. The analysis has been performed taking into account the 1st, 2nd, 4th, 6th and 8th modes. (a) Plot for all the possible damage position and (b) zoom nearest the minimum point.

To describe in a more realistic way the unavoidable measurement noise that affects the experimental data, a set of different realisations of pseudo-experimental frequencies has been considered. Namely, the noise has been introduced by defining for each sample the pseudo-experimental natural frequencies as follows:

$$\omega_i^D = \omega_{i,e}^D + R\gamma \tag{4}$$

where R is the level of noise and γ is a random variable, whose values are uniformly distributed between -1 and 1 with zero mean and independent from each other. In detail, 100 samples of noise simulations have been considered, which have been analysed by means of two different approaches.

The first approach implements the damage detection method discussed in Section 2.1 to each single simulation and investigates the influence of noise by evaluating the average mean error (AME_s) and the average standard deviation (ASD_s) of the position and the average mean error (AME_p) and the average standard deviation (ASD_p) of the level of damage obtained for an increasing number of samples [39]. The investigation has been performed evaluating the effect of three different parameters: the position of damage, the notch depth and the noise level.

In Figure 7, the AME_s , ASD_s , AME_p and ASD_p have been plotted for an increasing number of samples, fixing the notch depth (i.e. $p = 6$ cm and a noise level R equal to 0.2 Hz). Figure 7 shows that varying the position of damage, the proposed method is able to accurately evaluate the notch depth; in fact, the average mean error and the average standard deviation of the notch depth are very small, that is, the notch depth is correctly estimated and there is no dispersion of data.

It must be underlined that also in the worst case (damage localised at a distance of approximately 1/5 of the span length from the beam-to-column joints, which turns out an average mean error higher than the other examined cases), the average mean error of the notch depth is lower than $\Delta p = 2$ cm, which has been assumed as the step for discretising the damage steps and can therefore be considered as a measure of the accepted error.

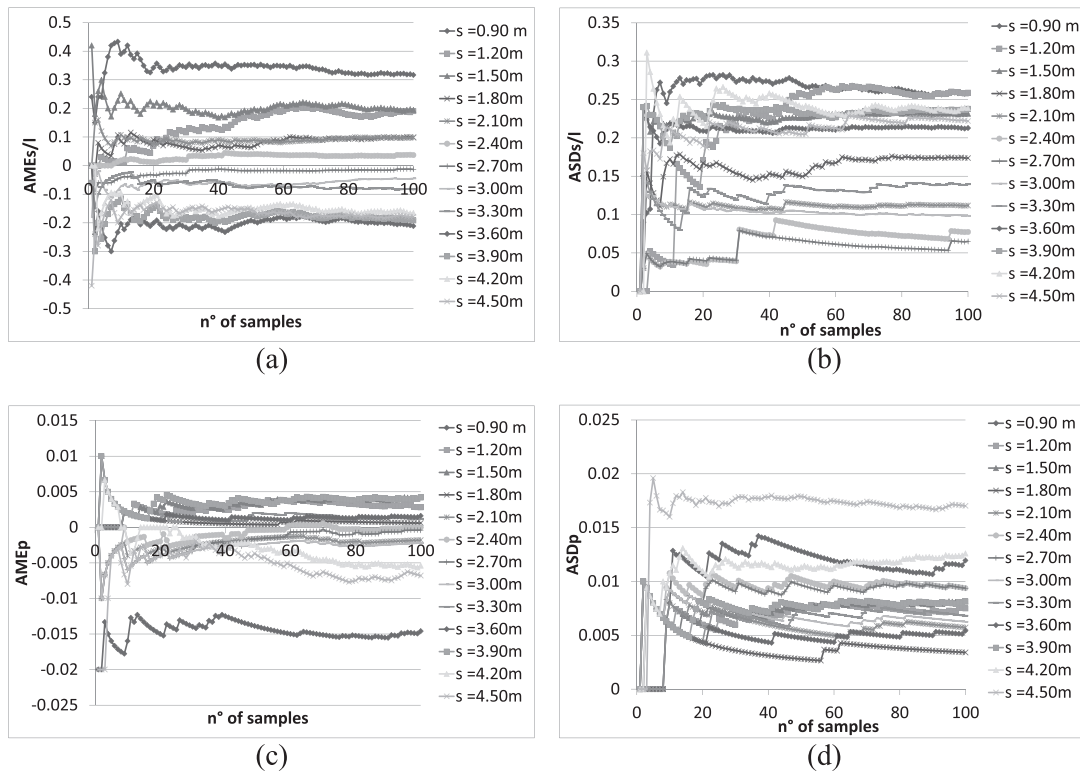


Figure 7. Influence of noise on the accuracy of the damage detection procedure varying the damage position and assuming $p = 6$ cm and $R = 0.2$ Hz: (a) average mean error of the position (AME_s), (b) average standard deviation of the position (ASD_s), (c) average mean error of the notch depth (AME_p) and (d) average standard deviation of the notch depth (ASD_p).

Similarly, also, the notch position is estimated with good accuracy, considered that the database has been defined discretising the beams with a step $\Delta s \cong 30$ cm, that is, 6% of the span length, which represents therefore the intrinsic-accepted error.

However, the accuracy of the identified position decreases when the damage is localised at a distance of about 1/5 of the span length from the beam-to-column joints; this circumstance can be justified observing that the local modes, which have been taken into account for the evaluation of the error function, show a lower variation of the related frequencies in these cases (Figure 2).

In Figure 8, the aforementioned parameters have been evaluated fixing the damage position (i.e. $s = 2.10$ m) and the level of noise (i.e. $R = 0.2$ Hz) and varying the notch depth. It can be observed that the average mean error decreases for an increasing damage level, and in all the examined cases, the notch depth is estimated with very high accuracy.

Similar results have been found also with reference to the estimation of the damage position.

In Figure 9, the same damaged cases are plotted taking into account an increased noise level, that is, $R = 0.4$ Hz; also in this case, the accuracy is good, except for the lower damage level; in this case, in fact, the natural frequencies show small variations, and the influence of noise is higher.

The aforementioned results have suggested to the writers a possible way to improve the accuracy of the procedure, by performing the error minimisation not on a single test but on a sort of 'average' test. In detail, the error function has been evaluated by adding the error functions evaluated for each one of the considered simulated tests, for an increasing number of tests, and applying the error minimisation procedure to the 'average' error function.

In Figure 10, the errors in the estimated damage position and in the notch depth are plotted, respectively, for the same damaged cases as in Figure 7 and for an increasing number of samples. It can be observed that for all the possible damage positions, the notch depth is exactly estimated, while the damage position can be exactly or almost exactly evaluated if at least five to six tests are included in the average. An exception is represented by the damage localised at a distance around 90 cm from

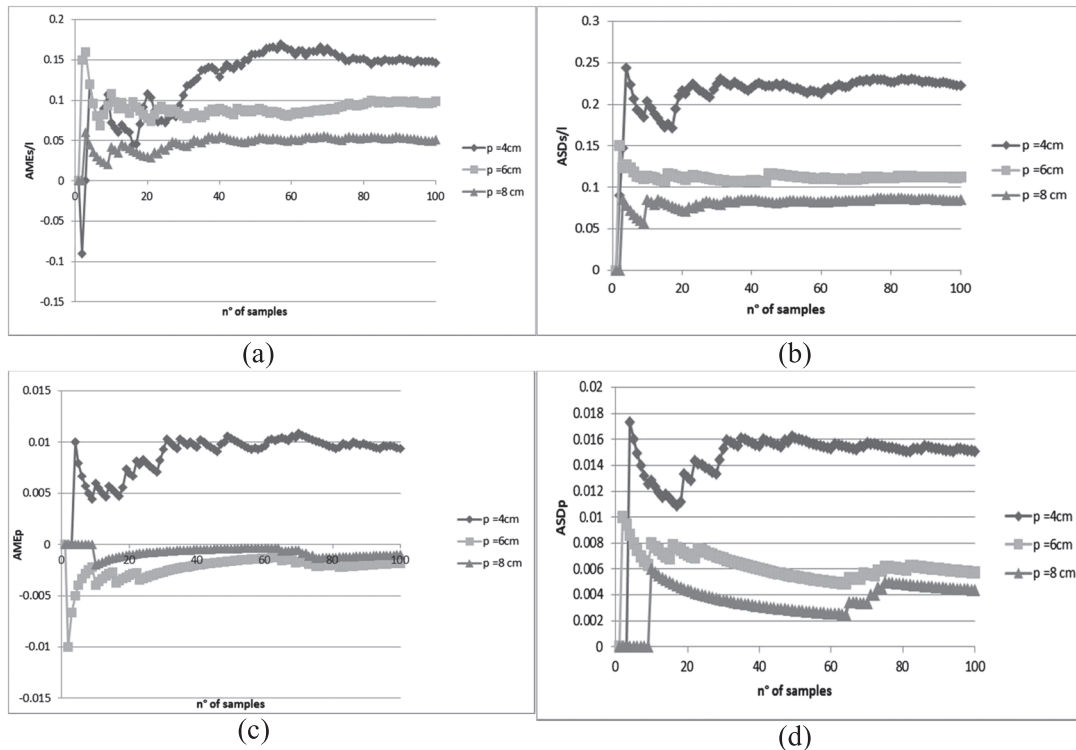


Figure 8. Influence of noise on the accuracy of the damage detection procedure, varying the damage level and assuming $s = 2.10$ m and $R = 0.2$ Hz: (a) average mean error of the position (AME_s), (b) average standard deviation of the position (ASD_s), (c) average mean error of the notch depth (AME_p) and (d) average standard deviation of the notch depth (ASD_p).

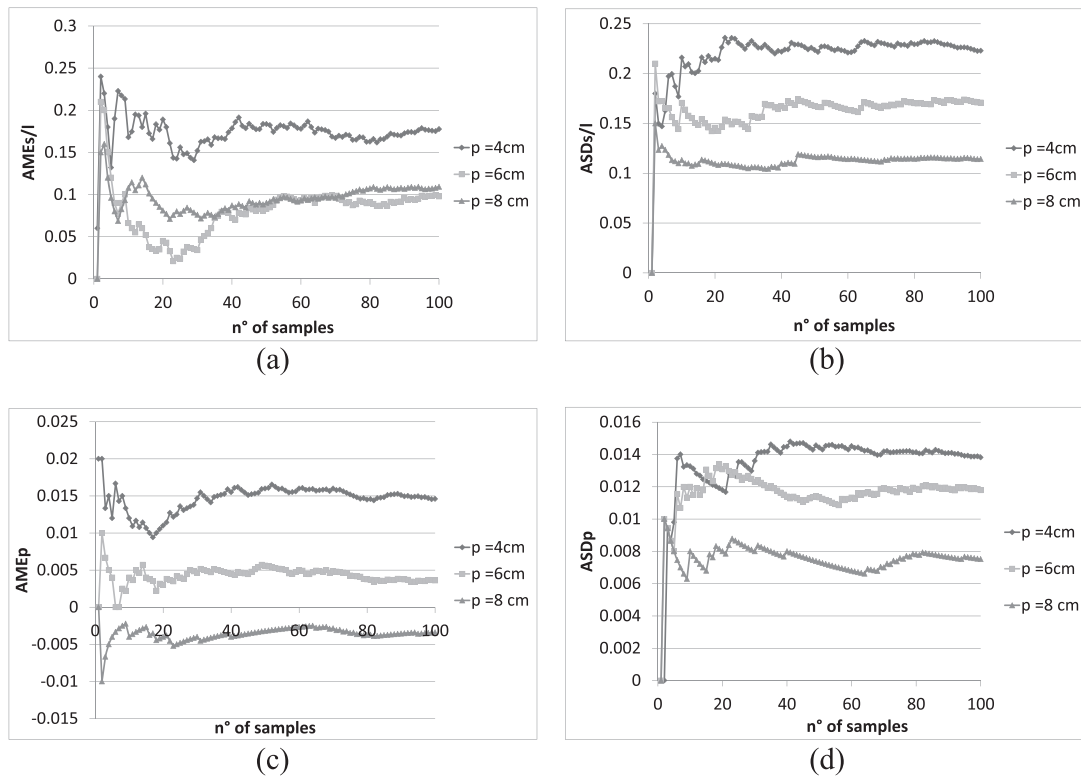


Figure 9. Influence of noise on the accuracy of the damage detection procedure varying the damage level and assuming $s = 2.10$ m and $R = 0.4$ Hz: (a) average mean error of the position (AME_s), (b) average standard deviation of the position (ASD_s), (c) average mean error of the notch depth (AME_p) and (d) average standard deviation of the notch depth (ASD_p).

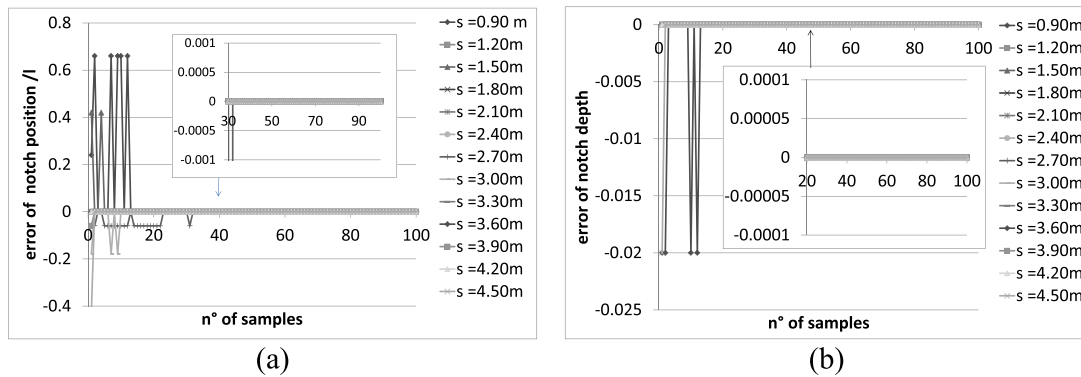


Figure 10. Influence of noise on the accuracy of the damage detection procedure, applied to the same cases in Figure 7 (i.e. $p = 6$ cm and $R = 0.2$ Hz, for different damage positions) by means of the ‘average’ error function introduced in Section 3.1: (a) error in the estimated damage position versus the number of considered tests and (b) error in the estimated damage level versus the number of considered tests.

the beam-to-column joint, and in fact, in this case, the variations of the natural frequencies (Figure 2) are lower than the other possible locations of damage. However, the result of the procedure can be improved by considering higher order modes, that is, modes that show significant frequencies variations for damage localised in the aforementioned position.

The analysis has also been performed investigating the damaged cases of Figure 8, that is, evaluating the influence of different notch depths: it can be observed that reducing the damage level, the

accuracy of the procedure does not vary if the error function is evaluated taking into account at least five to six tests (Figure 11).

The same considerations can be done also in the cases of Figure 12, which shows the damage position and level errors for the same cases of Figure 11 but with a noise level double of that in the previous case.

3.2. Sample case #2: three-span and three-floor steel planar frame

To test the performance and robustness of the proposed technique in evaluating the position and the severity of damage, a numerical simulation has been carried out on a more complex planar frame. In detail, the three-storey and three-bay steel plane frame structure, shown in Figure 13, has been considered.

As in previous examples, the total mass is the sum of the self-weight and of the non-structural mass, the latter described in Section 3.1. The frame has been discretised into 240 beam-column elements around 30-cm long, with 240 nodes.

The main information on the FE model of the frame is shown in Figure 13. As in the previous case (Section 3.1), the columns are fully fixed at the base, the beam-column connections have been assumed as rigid and the damping coefficient is equal to 0.5%.

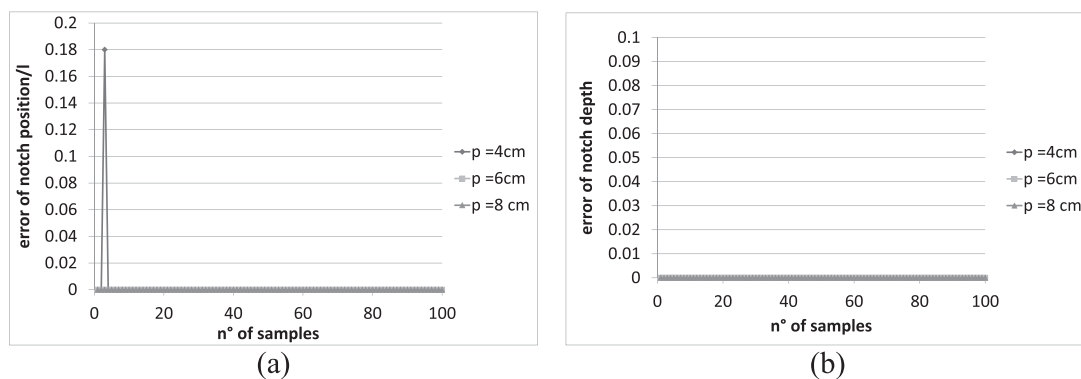


Figure 11. Influence of noise on the accuracy of the damage detection procedure, applied to the same cases in Figure 8 (i.e. $s=2.10$ m and $R=0.2$ Hz, for different damage levels) by means of the 'average' error function introduced in Section 3.1: (a) error in the estimated damage position versus the number of considered tests and (b) error in the estimated damage level versus the number of considered tests.

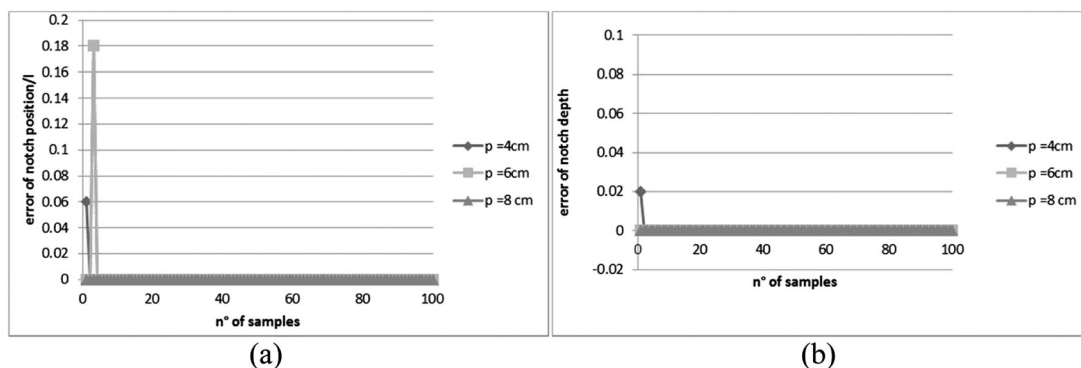


Figure 12. Influence of noise on the accuracy of the damage detection procedure, applied to the same cases in Figure 9 (i.e. $s=2.10$ m and $R=0.4$ Hz, for different damage levels) by means of the 'average' error function introduced in Section 3.1: (a) error in the estimated damage position versus the number of considered tests and (b) error in the estimated damage level versus the number of considered tests.

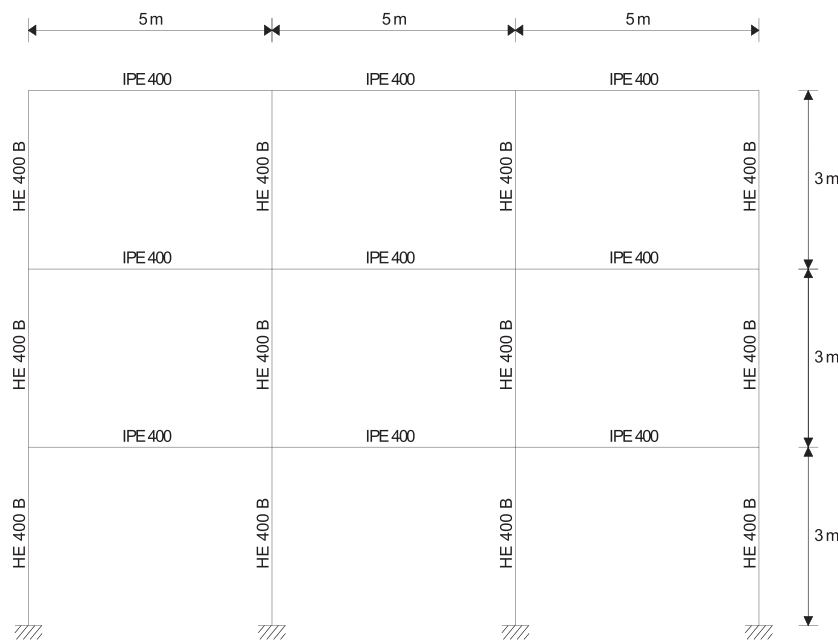


Figure 13. Steel frame of Section 3.2. For each floor, added mass 2850 kg/m. In the finite element model, damping coefficient 0.5 %.

The first 12 mode shapes and natural frequencies of the frame structure are shown in Figure 14. It can be observed that the first, second and tenth modes are related to ‘global’ modes, while the others are ‘local’ modes.

As in the previously examined case, damage is defined as a reduction of the transversal section of a beam with non-significant mass variation.

Seventeen levels of damage have been considered and described in the FE model through rotational spring, whose stiffness has been calculated in accordance with Chondros *et al.* [48] (see also Eqn 2); in Table I, the stiffness of the equivalent rotational spring k is reported for different notch depths p .

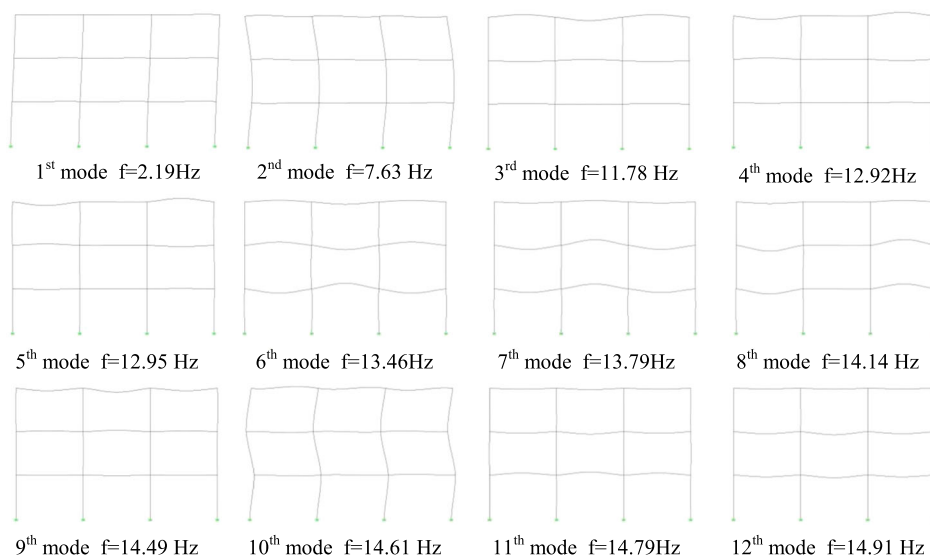


Figure 14. First 12 natural modes of the undamaged frame of Figure 13.

Table I. Parameters of the rotational spring equivalent to a notch in an IPE 400 beam (see frame in Figure 13).

| # Spring | p (cm) | p/h | K(GNm) |
|----------|----------|-------|--------|
| 1 | 10 | 0.25 | 20.9 |
| 2 | 9.5 | 0.24 | 24.3 |
| 3 | 9 | 0.23 | 28.2 |
| 4 | 8.5 | 0.21 | 32.9 |
| 5 | 8 | 0.20 | 38.4 |
| 6 | 7.5 | 0.19 | 45 |
| 7 | 7 | 0.18 | 53 |
| 8 | 6.5 | 0.16 | 62.8 |
| 9 | 6 | 0.15 | 75.1 |
| 10 | 5.5 | 0.14 | 90.8 |
| 11 | 5 | 0.13 | 111.1 |
| 12 | 4.5 | 0.11 | 138.4 |
| 13 | 4 | 0.10 | 175.9 |
| 14 | 3.5 | 0.09 | 229.9 |
| 15 | 3 | 0.08 | 311.7 |
| 16 | 2.5 | 0.06 | 445.1 |
| 17 | 2 | 0.05 | 686.3 |

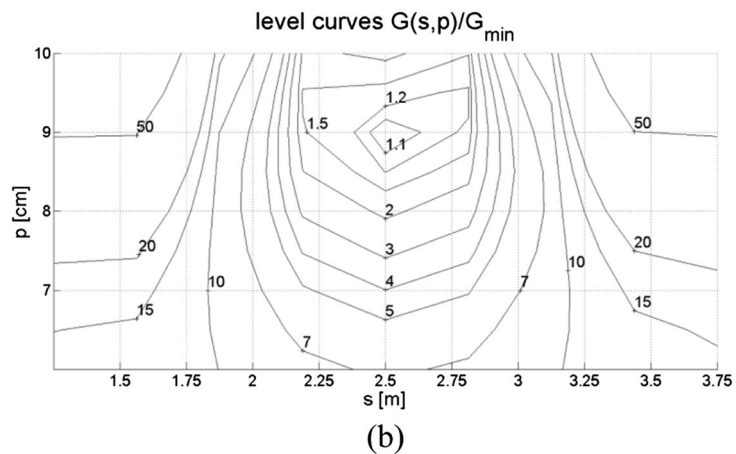
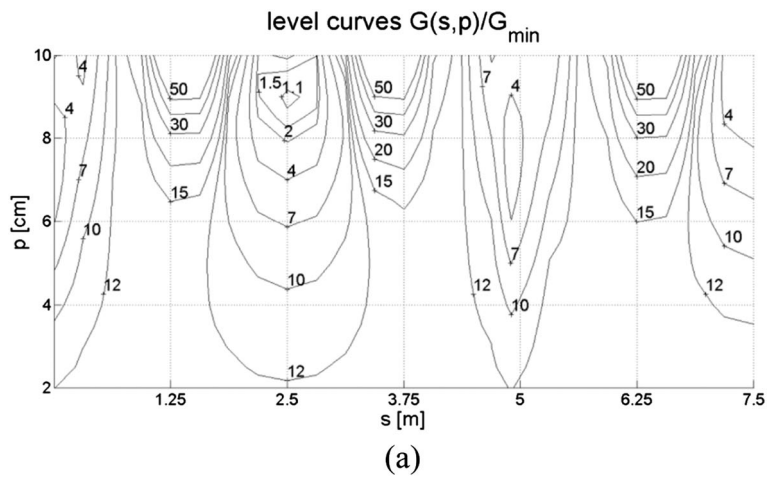


Figure 15. Normalised error function G/G_{\min} for the frame in Figure 13, pseudo-experimental data generated with damage $s=2.5$ m and $p=9$ cm. The analysis has been performed taking into account the 3rd, 4th, 11th and 13th modes: (a) level curves for all the possible damage position and (b) zoom nearest the minimum point.

As an example, a single notch in a beam of the second floor has been considered. Thus, varying the position of the damage through the nodes of the beams at the second floor, a database of the frequencies of the first 20 natural modes has been built for 17 levels of damage.

According to the procedure described in Section 2.1, the accuracy in the identification of the position and level of damage depends of course on the discretisation of the beams (nodes distance $\Delta s \approx 30$ cm, that is, 1/16 span) and of the notch ($\Delta p \approx 0.5$ cm), and Δs and Δp represent therefore an intrinsic error, which can be reduced only with a more dense discretisation and an higher calculation effort.

In the present example, however, an accuracy $\Delta s \approx 30$ cm and $\Delta p \approx 0.5$ cm has been considered as sufficient; even looking only for a damage at the second floor (that is just one step of the substructure approach here used) and taking into account the symmetry of the frame, the database includes in fact 425 damaged structures (25 nodes and 17 level of damage), whose analysis has required a huge effort.

However, an iterative procedure could be implemented for more complex structures that, after a preliminary identification of damage (position and severity) with a rough discretisation, improves the accuracy by means of a database more and more refined (smaller Δs and Δp) around the solution found in the previous steps.

As in Section 3.1, pseudo-experimental time histories (e.g. generated by numerical integration of the FE model) have been considered for the three-storey and three-bay frame of Figure 13.

For an impulsive force applied at 2/3 of the span of the second-floor beam, on the left side of the frame (Figure 13), the time histories of accelerations at structural nodes have been generated with a sampling frequency of 1000 Hz.

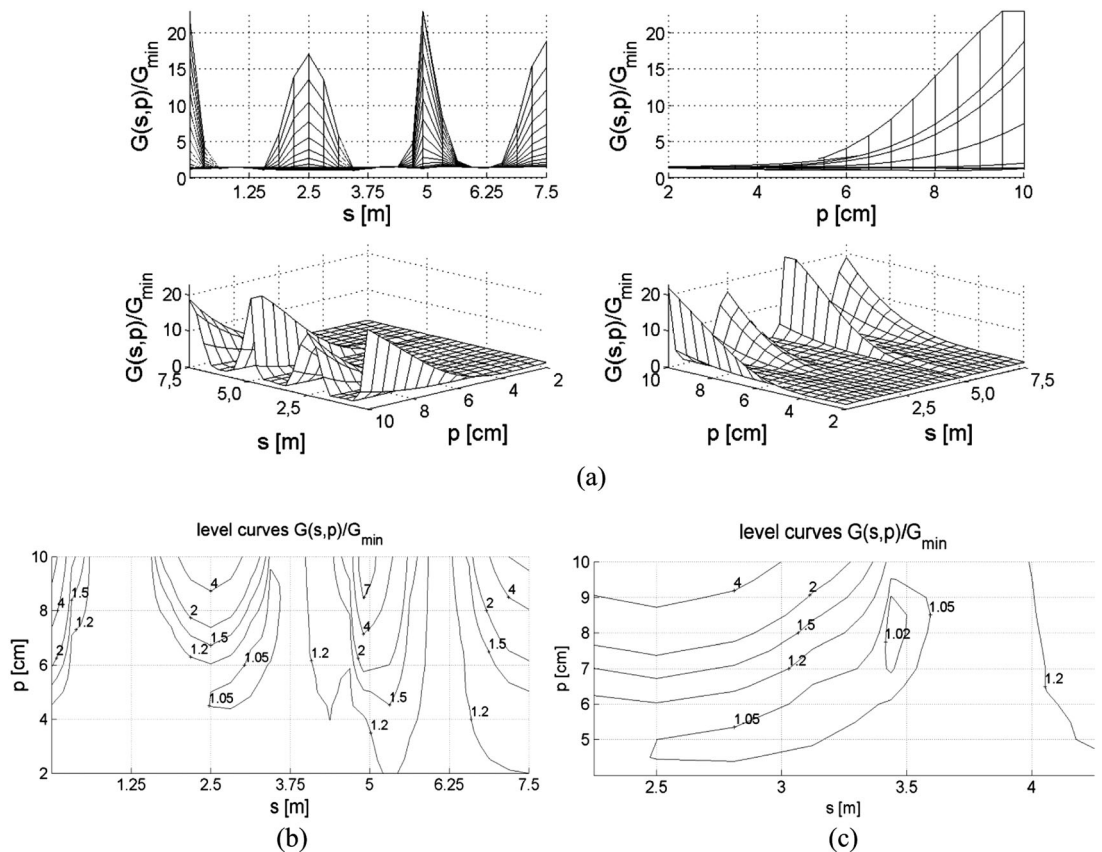


Figure 16. Normalised error function G/G_{min} for the frame in Figure 13, pseudo-experimental data generated with damage $s = 3.1$ m and $p = 7$ cm. The analysis has been performed taking into account the 3rd, 4th, 6th and 9th modes: (a) 3D view, (b) level curves for all the possible damage position and (c) zoom nearest the minimum point.

The pseudo-experimental data so obtained have been elaborated, and as in Section 3.1, the first six identified natural frequencies have been included in the error function of Eqn 1.

Three different damage cases have been examined: (i) a notch localised at 2.5 m from the left end of the second-floor beam and characterised by a depth equal to 9 cm; (ii) a notch localised at 3.1 m from the left end of the second-floor beam and characterised by a depth equal to 7 cm; and (iii) a notch localised at about 6.85 m from the left end of the second-floor beam and characterised by a depth equal to 6 cm. Figures 15–17 show the level curves of the error function for the aforementioned cases. The procedure is able to identify the position and severity of damage with good accuracy in the first examined configuration (Figure 15), while in the second damaged configuration (Figure 16), the position of damage is identified with an error of about 30 cm and the level of damage is identified with an error of about 1.5 cm ($3\Delta p$).

The reduced accuracy of this result is mainly due to the selection of the modes used in the damage detection analysis; in fact, no one of the considered local modes (third, fourth, sixth and ninth modes, see Figure 14) attains its maximum displacement in the damaged section (i.e. the section at 3.1 m from the left end of the second-floor beam), and this reduces the sensitivity of modal frequencies to damage. Analogous considerations could be done for the third damaged configuration (Figure 17), for which multiple solutions can be found, including the right one.

In the authors' opinion, in these cases, an improvement in the effectiveness of the procedure could also be obtained by modifying the error function with the introduction of modal assurance criterion (MAC)

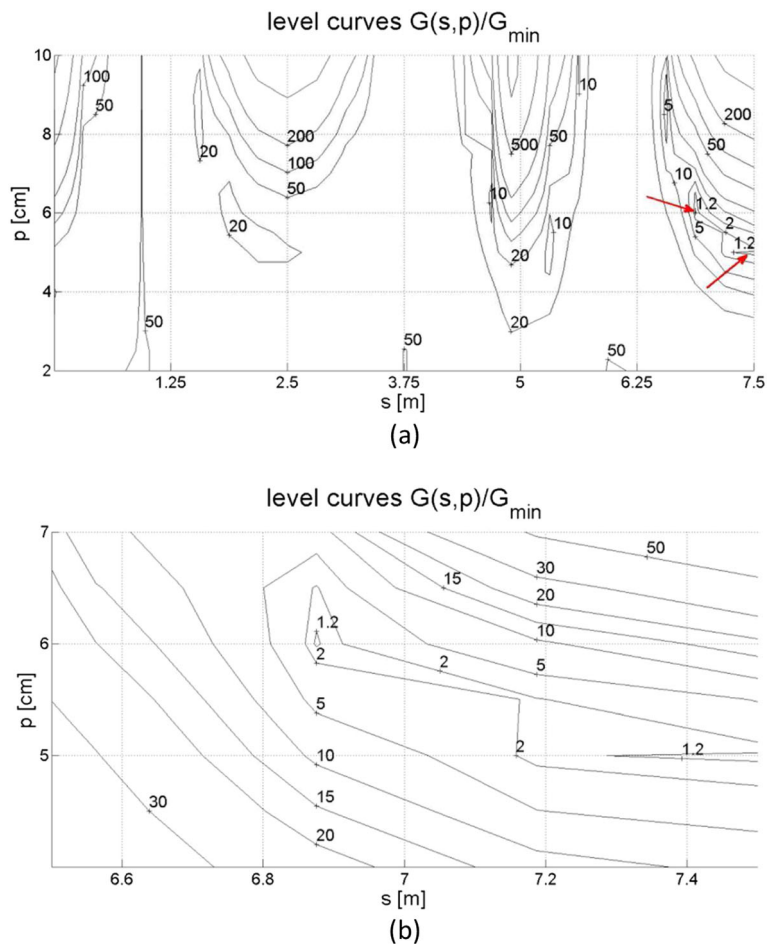


Figure 17. Normalised error function G/G_{min} for the frame in Figure 13, pseudo-experimental data generated with damage $s \approx 6.85$ m and $p = 6$ cm. The analysis has been performed taking into account the 3rd, 4th, 9th and 11th modes: (a) level curves for all the possible damage position and (b) zoom nearest the minimum point.

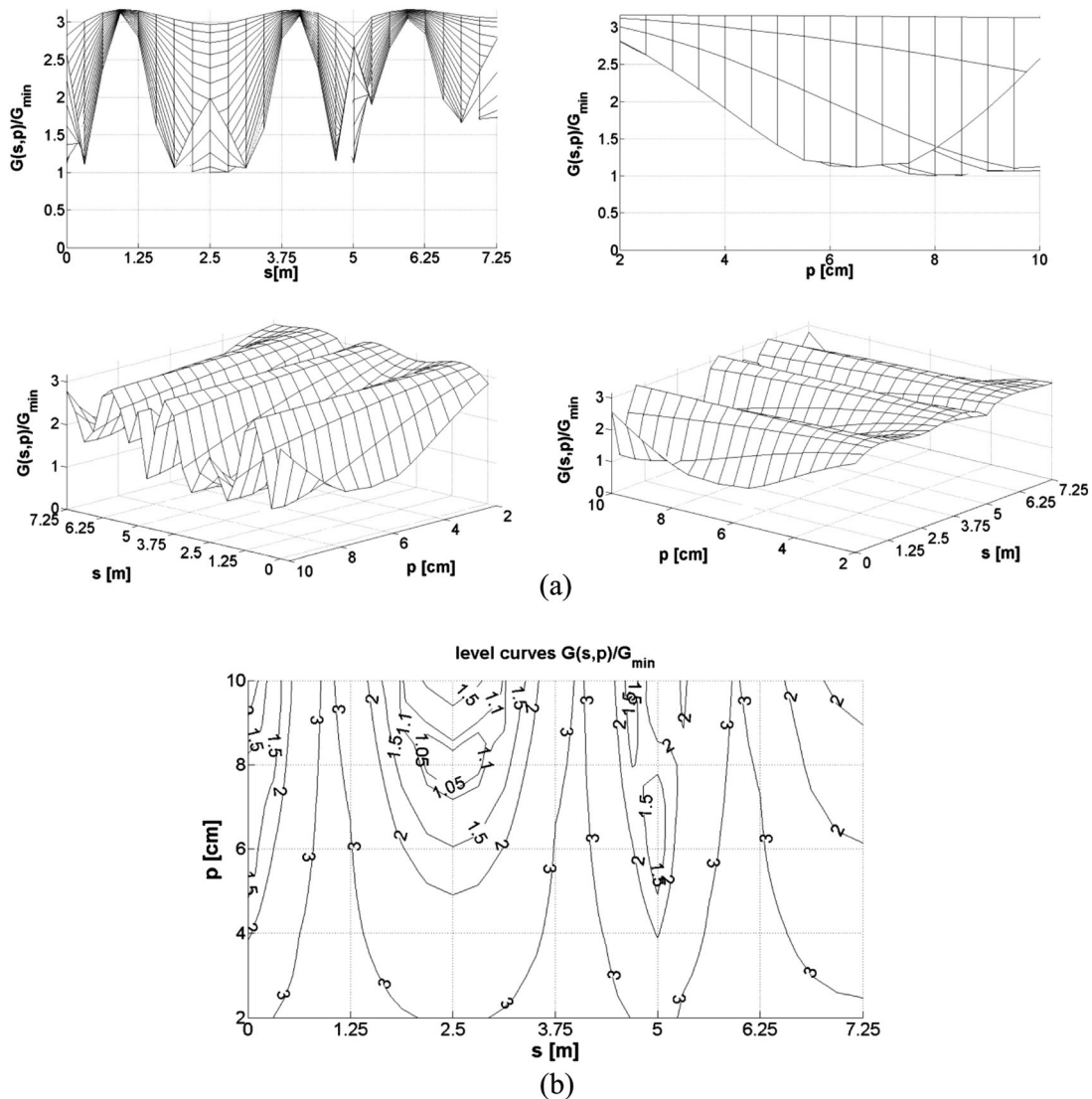


Figure 18. The frame in Figure 13, with damage $s = 2.5$ m and $p = 8$ cm. Mean error function G/G_{min} for 10 sample cases of pseudo-experimental data with maximum error on natural frequencies ranging within ± 0.2 Hz (random noise). The analysis has been performed taking into account the 3rd, 4th, 5th, 6th, 7th, 8th, 9th, 11th and 12th modes: (a) 3D view and (b) level curves.

number, and by a careful choice of the modes considered in the error function, which has to be implemented taking into account the sensitivity of the modes to the damage position; this will be the objective of a future research.

In the aforementioned cases, the influence of the noise has not been taken into account.

To verify also in this case the effectiveness of the approach, which allows to filter out measurement noise (assumed as random) by means of data redundancy, two damaged configurations have been examined: (i) a notch localised at 2.5 m from the left end of the second-floor beam and characterised by a depth equal to 8 cm and (ii) a notch localised at about 6.85 m from the left end of the second-floor beam and characterised by a depth equal to 7 cm. For each one of the aforementioned damaged configurations and starting from the pseudo-experimental frequencies of the FE database, 10 different random sequences of noise, described by an error ranging within ± 0.2 Hz, have been considered, and the error function has been evaluated as described for the cases in Figures 10–12. In Figures 18 and 19, the results of the proposed procedure are shown for an increasing number of samples. Because of the random

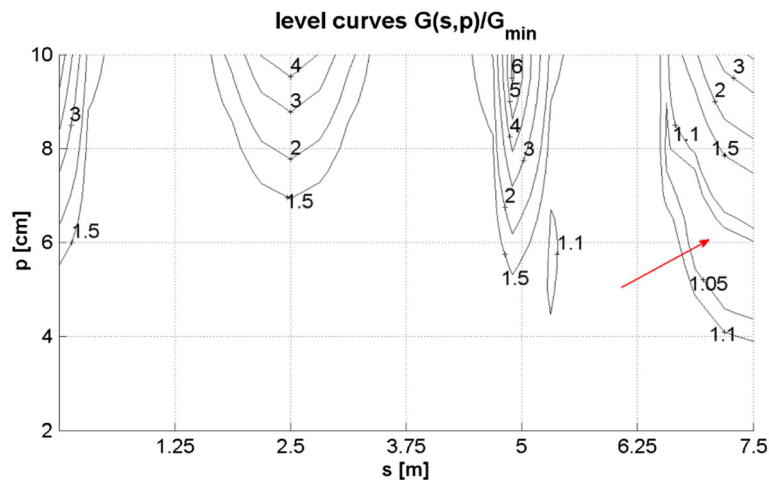


Figure 19. The frame in Figure 13, with damage $s \cong 6.85$ m and $p = 7$ cm. Mean error function G/G_{\min} for 10 sample cases of pseudo-experimental data with maximum error on natural frequencies ranging within ± 0.2 Hz (random noise). The analysis has been performed taking into account the 3rd, 4th, 5th, 6th, 7th, 8th, 9th, 11th and 12th modes: level-curves.

nature of the error, its effect on the value of the error functions is reduced by the averaging procedure, and the results of the damage detection are quite accurate.

4. CONCLUDING REMARKS

The paper investigates the possibility of identifying localised damages for linear elastic frames using only natural frequencies measured in the undamaged and damaged configurations.

It identifies the position and severity of damage by using a database of FE models simulating a wide range of variation of such parameters and whose effectiveness has been experimentally proven for multi-span beams [41,42].

In this paper, multi-span and multi-floor framed structures are considered and analysed by means of a substructure approach; the basic idea is that in this case, the FE database of damaged models, to be used in the minimization of the error function, must refer to the natural frequencies of the local modes of substructures, that is, the only modes significantly affected by the localised damage considered here.

Such a substructure approach, applied in Section 3.1 to a two-span and two-floor frame, shows [41,42] an accuracy comparable with the case of a multi-span single beam. Numerical investigation on a three-span and three-floor frame (Section 3.2) also shows an acceptable accuracy.

The effectiveness of the method is evaluated also taking into account the influence of measurement noise, which has been modelled as a random variable with zero mean, uniformly distributed in a given range. In the case of significant measurement noise, the damage detection procedure allows an accurate result only if multiple sets of experimental frequencies (damaged and undamaged) are considered, in order to filter out such noise through redundant data.

However, as the substructure affected by damage is not known *a priori*, a drawback of the procedure is that each substructure has to be controlled through a suitable distribution of the sensors, which could imply a huge computational burden for an increasing structural complexity, because of the corresponding growth of the possible damaged configurations. In this case, the implementation of an automatic algorithm to build the database of damaged–undamaged frequencies is mandatory, and this will be dealt with in future developments of this research.

Also, the practical applicability of the substructure approach to multi-storey frames, so far explored only by means of numerical data (pseudo-experimental), will certainly require an experimental validation in the future, at least to the laboratory scale.

ACKNOWLEDGEMENTS

This work has been partially funded by grants from University “G. D’Annunzio” of Chieti-Pescara, Faculty of Architecture (MURST ex 60%, 2008). Dr Gabriele Bellizzotti, a former PhD student of V.S. [42] and co-author for other papers [41,43] of the writers, is deeply acknowledged. The PRIN-MIUR 2010 research project entitled ‘Dynamics, Stability and Control of Flexible Structures’ is also acknowledged.

REFERENCES

1. Shi T, Jones NP, Ellis JH. Simultaneous estimation of system and input parameters from output measurements. *Journal of Engineering Mechanics* 2000; **126**(7):746–753.
2. Sepe V, Zingali AE. Wind induced response of an elevated steel water tank. *Wind and Structures* 2001; **4**(5):383–398.
3. Brincker R, Ventura CE, Andersen P. Why output-only modal testing is a desirable tool for a wide range of practical applications. *Proc. of the 21st IMAC*, Florida, USA, 2003.
4. Capecchi D, De Angelis M, Sepe V. Modal model identification with unknown nonstationary base motion. *Meccanica* 2004; **39**:31–45.
5. Carusi P, Sepe V, Viskovic A. Techniques of structural identification for the monitoring of historical buildings: first experimental results for a masonry tower, *Proceedings of SAHC4-Structural analysis of historical constructions - Possibilities of numerical and experimental techniques*, Padova, Italy, 2004; **1**:461–467.
6. Sepe V, Capecchi D, De Angelis M. Modal model identification of structures under unmeasured seismic excitations. *Earthquake Engineering & Structural Dynamics* 2005; **34**:807–824.
7. Sepe V, Vestroni F, Vidoli S, Mele R, Tisalvi M. Train-induced vibrations of masonry railway bridges. *Proc. of the 6th European Conference on Structural Dynamics EURODYN* 2005, Paris, France, **1**:161–166.
8. Zhang L, Brincker R, Andersen P. An overview of operational modal analysis: major development and issues. *Proc. of the 1st IOMAC*, Copenhagen, Denmark, 2005.
9. Perry MJ, Koh CG. Output-only structural identification in time domain: numerical and experimental studies. *Earthquake Engineering & Structural Dynamics* 2007; **37**:517–533.
10. Benedettini F, Gentile C. Ambient vibration testing and operational modal analysis of a masonry tower. *Proc. of the 2nd IOMAC*, Copenhagen, Denmark, 2007.
11. Diaferio M, Foti D, Sepe V. Dynamic identification of the tower of the Provincial Administration Building, Bari, Italy. *Proc. of the Eleventh International Conference on Civil, Structural and Environmental Engineering Computing*, Civil-Comp 2007, Malta, 2007.
12. Gentile C, Gallino N. Condition assessment and dynamic system identification of a historic suspension footbridge. *Structural Control and Health Monitoring* 2008; **15**(3):369–388.
13. Andersen P, Brincker R, Ventura C, Cantieni R. Mode estimation of civil structures subject to ambient and harmonic excitation. *Proceedings of the 26th International Modal Analysis Conference (IMAC)*, Orlando, Florida USA, 2008.
14. Brincker R. History of Civil Engineering Modal Analysis: IMAC Keynote. *Proc. of the IMAC-XXVI: Conference & Exposition on Structural Dynamics - Technologies for Civil Structures*, Garden Grove, California USA, 2008.
15. Diaferio M, Foti D, Giannoccaro NI. Non-destructive characterization and identification of the modal parameters of an old masonry tower. In *Proc. 2014 6th IEEE Workshop on Environmental, Energy and Structural Monitoring Systems*, EEMS Naples, Italy, September 17–18, 2014.
16. Diaferio M, Foti D, Giannoccaro NI. Identification of the modal properties of an instrumented building. In *Proc. IOMAC 2009 -3rd International Operational Modal Analysis Conference*, Portonovo; Italy, 2014; 357–364.
17. Diaferio M, Foti D, Giannoccaro NI, Ivorra S. Optimal model through identified frequencies of a masonry building structure with wooden floors. *International Journal of Mechanics* 2014; **8**:282–288.
18. Diaferio M, Foti D, Gentile C, Giannoccaro NI, Saisi A. Dynamic testing of a historical slender building using accelerometers and radar. In *Proc. IOMAC15 – 6th International Operational Modal Analysis Conference, Gijón, Spain 2015*, paper 153.
19. Gentile C, Saisi A. FE modeling of a historic masonry tower and vibration-based systematic model tuning. *Advanced Materials Research* 2010; **133-134**:435–440.
20. Gangone MV, Whelan MJ, Janoyan KD. Wireless monitoring of a multi-span bridge superstructure for diagnostic load testing and system identification. *Computer-Aided Civil and Infrastructure Engineering* 2011; **26**(7):560–579.
21. Benedettini F, Gentile C. Operational modal testing and FE model tuning of a cable-stayed bridge. *Engineering Structures* 2011; **33**(6):2063–2073.
22. Diaferio M, Foti D, Mongelli M, Giannoccaro IN, Andersen P. Operational modal analysis of a historical tower in Bari. *Conference Proceedings of the Society for Experimental Mechanics Series, “IMAC XXIX”*, Jacksonville, Florida, USA 2011; **4**:335–342.
23. Antonacci E, De Stefano A, Gattulli V, Lepidi M, Matta E. Comparative study of vibration-based parametric identification techniques for a three-dimensional frame structure. *Structural Control and Health Monitoring* 2012; **19**(5):579–608.
24. Foti D, Diaferio M, Giannoccaro IN, Mongelli M. Ambient vibration testing, dynamic identification and model updating of a historic tower. *NDT & E International* 2012; **47**:88–95.
25. Basu B. Identification of stiffness degradation in structures using wavelet analysis. *Construction and Building Materials* 2005; **19**:713–721.
26. Goggins J, Broderick BM, Basu B, Elghazouli AY. Investigation of the seismic response of braced frames using wavelet analysis. *Structural Control and Health Monitoring* 2007; **14**(4):627–648.
27. Nagarajaiah S, Basu B. Output only modal identification and structural damage detection using time frequency and wavelet techniques. *Earthquake Engineering and Engineering Vibration* 2009; **8**(4):583–605.
28. Basu B, Nagarajaiah S, Chakraborty V. Online identification of linear time-varying stiffness of structural systems by wavelet analysis. *Structural Health Monitoring* 2008; **7**(1):21–36.
29. Moaveni B, Conte JP, Hemez FM. Uncertainty and sensitivity analysis of damage identification results obtained using finite element model updating. *Computer-Aided Civil and Infrastructure Engineering* 2009; **24**(5):320–334.

30. Chellini G, De Roeck G, Nardini L, Salvatore W. Damage detection of a steel-concrete composite frame by a multilevel approach: experimental measurements and modal identification. *Earthquake Engineering & Structural Dynamics* 2008; **37**(15):1763–1783.
31. Savadkoobi AT, Molinari M, Bursi OS, Friswell MI. Finite element model updating of a semi-rigid moment resisting structure. *Structural Control and Health Monitoring* 2011; **18**:149–168.
32. Xiaodong J, Jiaru Q, Longhe X. Damage diagnosis of a two-storey spatial steel braced-frame model. *Structural Control and Health Monitoring* 2007; **14**:1083–1100.
33. Amani MG, Riera JD, Curadelli RO. Identification of changes in the stiffness and damping matrices of linear structures through ambient vibrations. *Structural Control and Health Monitoring* 2007; **14**:1155–1169.
34. Ramos L, De Roeck G, Lourenço P, Campos-Costa A. Damage identification on arched masonry structures using ambient and random impact vibrations. *Engineering Structures* 2010; **32**(1):146–162.
35. Rahai A, Bakhtiari-Nejad F, Esfandiari A. Damage assessment of structure using incomplete measured mode shapes. *Structural Control and Health Monitoring* 2007; **14**:808–829.
36. Lee U, Shin J. A frequency domain method of structural damage identification formulated from the dynamic stiffness equation of motion. *Journal of Sound and Vibration* 2002; **257**(4):615–634.
37. Salawu OS. Detection of structural damage through changes in frequency: a review. *Engineering Structures* 1997; **19**(9):718–723.
38. Morita K, Teshigawara M, Hamamoto T. Detection and estimation of damage to steel frames through shaking table tests. *Structural Control and Health Monitoring* 2005; **12**:357–380.
39. Greco A, Pau A. Damage identification in Euler frames. *Computers and Structures* 2012; **92-93**:328–336.
40. Pau A, Greco A, Vestroni F. Numerical and experimental detection of concentrated damage in a parabolic arch by measured frequency variations. *Journal of Vibration and Control* 2010; **17**(4):605–614.
41. Sepe V, Bellizzotti G, Diaferio M. Identification of local damage in beams and frames. *Proc. of the 19th Conf. Italian Association for Theoretical and Applied Mech AIMETA09*, Ancona, Italy, 2009.
42. Bellizzotti G. Dynamic identification of structures and damage identification by means of non destructive dynamical tests. PhD Thesis, University “G. D’Annunzio” of Chieti-Pescara, Italy (*in Italian*), 2009.
43. Sepe V, Bellizzotti G. Identification of damage in structural elements not directly accessible. *Proc. of the 3rd IOMAC*, Portonovo-Ancona, Italy, 2009.
44. Xia Y, Hao H. Measurement selection for vibration-based structural damage identification. *Journal of Sound and Vibration* 2000; **236**(1):89–04.
45. Kögl M, Hurlbauss S, Gaul L. Finite element simulation of non-destructive damage detection with higher harmonics. *NDT & E International* 2004; **37**(3):195–205.
46. Douka E, Hadjileontiadis LJ. Time–frequency analysis of the free vibration response of a beam with a breathing crack. *NDT & E International* 2005; **38**(1):3–10.
47. Loutridis S, Douka E, Hadjileontiadis LJ. Forced vibration behaviour and crack detection of cracked beams using instantaneous frequency. *NDT & E International* 2005; **38**(5):411–419.
48. Chondros TG, Dimarogonas AD. A continuous cracked beam vibration theory. *Journal of Sound and Vibrations* 1998; **215**(1):17–34.